

Coupled channel study of a_0 resonances

Agnieszka Furman and Leonard Leśniak

*Henryk Niewodniczański Institute of Nuclear Physics,
PL 31-342 Kraków, Poland*

November 10, 2018

Abstract

The coupled channel model of the $a_0(980)$ and $a_0(1450)$ resonances has been constructed using the separable $\pi\eta$ and $K\bar{K}$ interactions. We have shown that two S-matrix poles corresponding to the $a_0(980)$ meson have significantly different widths in the complex energy plane. The $K\bar{K}$ to $\pi\eta$ branching ratio, predicted in our model near the $a_0(1450)$ mass, is in agreement with the result of the Crystal Barrel Collaboration. The $K\bar{K}$ interaction in the S-wave isovector state is *not* sufficiently attractive to create a bound $a_0(980)$ meson.

1 Introduction

Properties of scalar mesons are intensively studied in many theoretical and experimental articles [1–3]. The number of known isovector resonances in the scalar meson sector is smaller than the corresponding number of isoscalar resonances since only two isospin $I = 1$ states $a_0(980)$ and $a_0(1450)$ are listed in the last edition of the Review of Particle Physics [4]. The $a_0(980)$ state lies close to the $K\bar{K}$ threshold which can strongly influence the resonance shape in the $\pi\eta$ main decay channel. By comparing results given in Refs. [5] and [6] one can notice some differences in experimental determinations of the $a_0(980)$ mass and particularly of its width. More important mass and width differences of the $a_0(1450)$ state found in the $p\bar{p}$ annihilation by the Crystal Barrel Collaboration [6] and by the OBELIX Collaboration [7] have been pointed out by Montanet [3].

Internal structure of scalar mesons is not yet well understood. Many conflicting view-points in which scalars are treated as $q\bar{q}$ or $q\bar{q}q\bar{q}$ states, two-meson

quasi-bound states and mixed states including glueballs coexist (see, for example, [8–13]).

The a_0 resonances decay mainly to $\pi\eta$ and $K\bar{K}$ channels and the $a_0(1450)$ decays also to $\pi\eta'(958)$ [14]. Studies of the decay channels are potentially a rich source of information about a dynamics of the meson–meson interactions. Unfortunately the $\pi\eta$ and the $K\bar{K}$ phase shifts in the scalar–isovector state have not been experimentally determined although in several production experiments partial wave analyses have been performed [5, 15, 16]. On the other hand these phase shifts or the meson–meson scattering amplitudes have been calculated using theoretical models [9, 17–19]. We should remark, however, that an experimental determination of the $\pi\eta$ phase shifts is more difficult than a derivation of the $\pi\pi$ phase shifts. In the second case a strong dominance of one pion exchange has helped to obtain the $\pi\pi$ scalar–isoscalar phase shifts from the amplitudes of the $\pi\pi$ production on nucleons using pion beams [20, 21].

Closeness of the $a_0(980)$ to the K^+K^- and $K^0\bar{K}^0$ thresholds and existence of other scalar meson $f_0(980)$ at a very similar mass make possible an isospin mixing of both resonant states. The physical consequences of this phenomenon have been recently presented by several authors [22–24]. Theoretical investigations have been stimulated by new experimental results from Novosibirsk and Frascati on the radiative ϕ decays into $a_0(980)\gamma$ and $f_0(980)\gamma$ [25–27]. A good experimental insight into the a_0 – f_0 mixing can be achieved when an experimental effective mass resolution is significantly better than the mass difference between the K^+K^- and $K^0\bar{K}^0$ thresholds (about 8 MeV). Such a good resolution is also needed to measure the width of the $a_0(980)$ meson with a sufficient precision.

In the present paper we use the separable potential model formulated in Ref. [28]. This is an extension of a similar two-channel model developed in Ref. [29] to describe the $\pi\pi$ and $K\bar{K}$ S-wave $I = 0$ channel in which the $f_0(500)$ meson has been found. The mass and width of the $f_0(500)$ meson have been obtained by finding an appropriate pole of the S-matrix in the complex energy plane. The $\pi\pi$ and $K\bar{K}$ experimental phase shifts served as input to fix the model parameters in the scalar–isoscalar sector.

A simple application of the same procedure to the S-wave $I = 1$ channels is not yet possible since we do not know experimental values of the $\pi\eta$ and $K\bar{K}$ phase shifts. We can, however, fix four model parameters to fit values of masses and widths of two known a_0 resonances and use some experimental information about the $K\bar{K}$ to $\pi\eta$ branching ratio for the $a_0(980)$ to determine the remaining free parameter of the minimal version of the coupled channel ($\pi\eta$ and $K\bar{K}$) model. This analytic and unitary model has only five independent parameters but using it one can calculate elastic and inelastic $\pi\eta$ and $K\bar{K}$ S-wave isovector

amplitudes, a_0 coupling constants to two channels and positions of different S-matrix poles in the complex energy plane including those poles which have not been postulated as the experimental input. One can also answer an interesting question whether the $K\bar{K}$ forces are sufficiently strong to create a bound $I = 1$ S-wave state. Despite of its simplicity the model has an attractive possibility to check, confront and even correct phenomenological results obtained by different experimental groups in studies of the a_0 production processes.

2 Theoretical model

Let us briefly describe our theoretical model [28]. We consider two channels $\pi\eta$ (label 1) and $K\bar{K}$ (label 2). The separable potentials describe interactions between mesons:

$$\langle \mathbf{p} | V_{ij} | \mathbf{q} \rangle = \lambda_{ij} g_i(p) g_j(q) , \quad i, j = 1, 2 , \quad (1)$$

where $\lambda_{ij} = \lambda_{ji}$ are the real coupling constants and g_i are the form factors in Yamaguchi's form:

$$g_i(p) = \sqrt{\frac{2\pi}{m_i}} \frac{1}{p^2 + \beta_i^2} . \quad (2)$$

In Eq. (2) m_i are the reduced masses, β_i are the range parameters and p is the relative momentum. The matrix T of the scattering amplitudes satisfies the coupled channel Lippmann–Schwinger equation:

$$\langle \mathbf{p} | T | \mathbf{q} \rangle = \langle \mathbf{p} | V | \mathbf{q} \rangle + \int \frac{d^3s}{(2\pi)^3} \langle \mathbf{p} | V | \mathbf{s} \rangle \langle \mathbf{s} | G | \mathbf{s} \rangle \langle \mathbf{s} | T | \mathbf{q} \rangle , \quad (3)$$

where T , V , G are 2×2 matrices. The elements of the diagonal matrix G of propagators are given by:

$$G_i(s) = \frac{1}{E - E_i(s) + i\epsilon} , \quad \epsilon \rightarrow 0+ , \quad (4)$$

where s is the relative momentum, E is the total energy and E_i are the channels energies. The T-matrix elements satisfying Eq. (3) can be written as

$$\langle \mathbf{p} | T_{ij} | \mathbf{q} \rangle = g_i(p) t_{ij} g_j(q) , \quad i, j = 1, 2 , \quad (5)$$

where the matrix t is expressed below:

$$t = (1 - \lambda I)^{-1} \lambda . \quad (6)$$

In this equation λ is the symmetric matrix of the coupling constants and I is the diagonal matrix of integrals:

$$I_{ii} = \int \frac{d^3 s}{(2\pi)^3} g_i(s) G_i(s) g_i(s) . \quad (7)$$

The determinant of $(1 - \lambda I)$, called the Jost function $D(E)$, can be written as a function of two channel centre of mass momenta k_1 and k_2 :

$$D(k_1, k_2) = D_1(k_1) D_2(k_2) - F(k_1, k_2) , \quad (8)$$

where

$$D_i(k_i) = 1 - \lambda_{ii} I_{ii}(k_i) , \quad i = 1, 2 , \quad (9)$$

and

$$F(k_1, k_2) = \lambda_{12}^2 I_{11}(k_1) I_{22}(k_2) . \quad (10)$$

The Jost function can be used to express all the S-matrix elements in the following way:

$$\begin{aligned} S_{11} &= \frac{D(-k_1, k_2)}{D(k_1, k_2)} , & S_{22} &= \frac{D(k_1, -k_2)}{D(k_1, k_2)} , \\ S_{12}^2 &= S_{11} S_{22} - \frac{D(-k_1, -k_2)}{D(k_1, k_2)} . \end{aligned} \quad (11)$$

The matrix of potentials has five parameters: two β_i and three independent λ_{ij} parameters, which must be determined from data. In a case when masses and widths of two a_0 resonances are known a calculation of four parameters is rather simple. The positions of resonances in the complex energy plane coincide with poles of the S-matrix elements and with zeroes of the Jost function $D(k_1, k_2)$. Thus four model parameters can be found by solving two complex equations:

$$D(k_1^r, k_2^r) = 0 \text{ and } D(k_1^R, k_2^R) = 0 , \quad (12)$$

where k_i^r and k_i^R denote the complex momenta in a channel i related to the complex energy positions of the $a_0(980)$ and $a_0(1450)$ resonances, respectively.

There exists an ambiguity in determination of the momenta since a given resonance energy $E_p = M - i\Gamma/2$ (M being a resonance mass and Γ its width) can correspond to more than one resonance position in the complex plane of two momenta k_1 and k_2 . The energy conservation relation is quadratic in momenta, thus resonances can be situated on different sheets labelled by signs of imaginary parts $Im k_1$ and $Im k_2$. For example, the $a_0(980)$ resonance can be located on sheets $-+$ or $--$, called sheets II or III, respectively.

3 Experimental input and model parameters

In [6] the $a_0(980)$ resonance production amplitudes have been parametrised using the K -matrix form reducing to the modified version of the Flatté formula [30]:

$$F_i(m) = \frac{Ng_i}{m_0^2 - m^2 - i(\rho_1 g_1^2 + \rho_2 g_2^2)}, \quad i = 1, 2, \quad (13)$$

where m is the $\pi\eta$ or $K\bar{K}$ effective mass, $\rho_i = 2k_i/m$ and N is a constant. Using the parameters fitted in [6]: $m_0 = (999 \pm 2)$ MeV, $g_1 = (324 \pm 15)$ MeV, and the ratio of coupling constants squared $r = g_2^2/g_1^2 = 1.03 \pm 0.14$ we have calculated the positions of two poles of $F_i(m)$ at

$$\begin{aligned} M_1 &= (1005 \pm 3) \text{ MeV}, \Gamma_1 = (49 \pm 7) \text{ MeV on sheet II } (-+) \\ \text{and } M_2 &= (985 \pm 7) \text{ MeV}, \Gamma_2 = (92 \pm 13) \text{ MeV on sheet III } (--). \end{aligned} \quad (14)$$

Let us note that the first pole is located above the $K\bar{K}$ threshold while the second pole lies below it and the widths are different by a factor of about two. Similar results with very different widths can be found for solution B obtained in [31] by the Crystal Barrel Collaboration. It can be shown that in the modified Flatté model the difference of two widths is approximately proportional to the $K\bar{K}$ coupling constant squared

$$\Gamma_2 - \Gamma_1 \approx g_2^2 \cdot \frac{4\text{Re}q_2}{m_0^2}, \quad (15)$$

where q_2 is the $K\bar{K}$ complex momentum corresponding to the pole on sheet III. Thus the widths of two poles have to be different. Here we should point out that some numbers in (14) do not coincide with the pole positions written in [6] (also the sheet numbers seem to be interchanged).

The original Flatté parametrisation has been used by the E852 Collaboration in the study of the reaction $\pi^- p \rightarrow \eta\pi^+\pi^- n$ measured at Brookhaven at 18.3 GeV/c [5]. The E852 Group has performed a fit of the observed $\eta\pi^+$ effective mass distribution and obtained the mass position $M_r = (1001.3 \pm 1.9)$ MeV, the ratio of coupling constants $R = 0.91 \pm 0.10$ and the value of dimensionless coupling constant $g_{\eta\pi} = 0.243 \pm 0.015$, corresponding to the $\eta\pi$ width $\Gamma_{\eta\pi} = 81$ MeV calculated at the M_r position. After an effective mass correction for a finite experimental resolution this value was reduced to 70 ± 5 MeV [5] which is equivalent to a reduction of the $\eta\pi$ coupling constant to $g_{\eta\pi} = 0.210 \pm 0.015$. Using this value of $g_{\eta\pi}$ and the above numbers of M_r and

R we have found positions of two poles at

$$\begin{aligned} M &= (1006 \pm 3) \text{ MeV}, \Gamma = (51 \pm 5) \text{ MeV} \text{ on sheet II } (-+) \\ \text{and } M &= (988 \pm 5) \text{ MeV}, \Gamma = (89 \pm 10) \text{ MeV} \text{ on sheet III } (--). \end{aligned} \quad (16)$$

These positions are in very good agreement with those calculated by us for the Crystal Barrel Collaboration parameters in (14). Let us remark that the parameters of the $a_0(980)$ meson cited in Table II [5] in the line labelled by E852(C) do not correspond to the pole position of the production amplitude, so M_r and Γ placed in that line should not be interpreted as the $a_0(980)$ resonance mass and its width.

The presence of two distinct poles related to the $a_0(980)$ meson means that in principle one has two options while fixing the model parameters using Eq. (12). At first we shall discuss the case when the $a_0(980)$ pole is located on sheet II at $M_1 - i\Gamma_1/2 = (1005 - 24.5i) \text{ MeV}$. We expect that the $a_0(1450)$ resonance lies on sheet III since it is located far from the $\pi\eta$ and $K\bar{K}$ thresholds. We take its mass as $M = 1474 \text{ MeV}$ and the width as $\Gamma = 265 \text{ MeV}$.

In the simplest version of our two channel model we need further experimental constraints to fix the fifth model parameter. We choose the range variable β_1 in the $\pi\eta$ channel as a free parameter to fit the $K\bar{K}$ to $\pi\eta$ branching ratio defined as

$$BR = \frac{\int_{m_2}^{m_{max}} \rho_2 |F_2(m)|^2 dm}{\int_{m_1}^{m_{max}} \rho_1 |F_1(m)|^2 dm}, \quad (17)$$

where m_1 and m_2 are lower bounds of the effective mass and m_{max} is its upper bound. Using the K-matrix model of Ref. [6] this ratio can be expressed as the ratio of the integrals over the transition cross section and over the $\pi\eta$ elastic cross section:

$$BR = \frac{\int_{m_2}^{m_{max}} \sigma_{\pi\eta \rightarrow K\bar{K}}(m) k_1 m dm}{\int_{m_1}^{m_{max}} \sigma_{\pi\eta}^{el}(m) k_1 m dm}. \quad (18)$$

The branching ratio calculated for the $a_0(980)$ resonance on sheet II is shown in Fig. 1. Here $m_1 = m_\pi + m_\eta$ and $m_2 = 2m_K$, where m_π , m_η and m_K are the pion, eta and kaon masses, respectively. We see that BR depends strongly on the upper bound m_{max} . In order to avoid a strong interference of the wide $a_0(1450)$ with the $a_0(980)$ resonance, the limits of m_{max} , shown in Fig. 1, do not exceed 1.05 GeV. This interference is particularly important in the $K\bar{K}$ channel so the integration over the $K\bar{K}$ invariant masses higher than 1.05 GeV would lead to a significant distortion of the $a_0(980)$ branching ratio.

The variation of the branching ratio with β_1 is correlated with the dependence of the interchannel coupling constant λ_{12} on β_1 . Maximum of λ_{12}^2 lies for β_1 near 20 GeV.

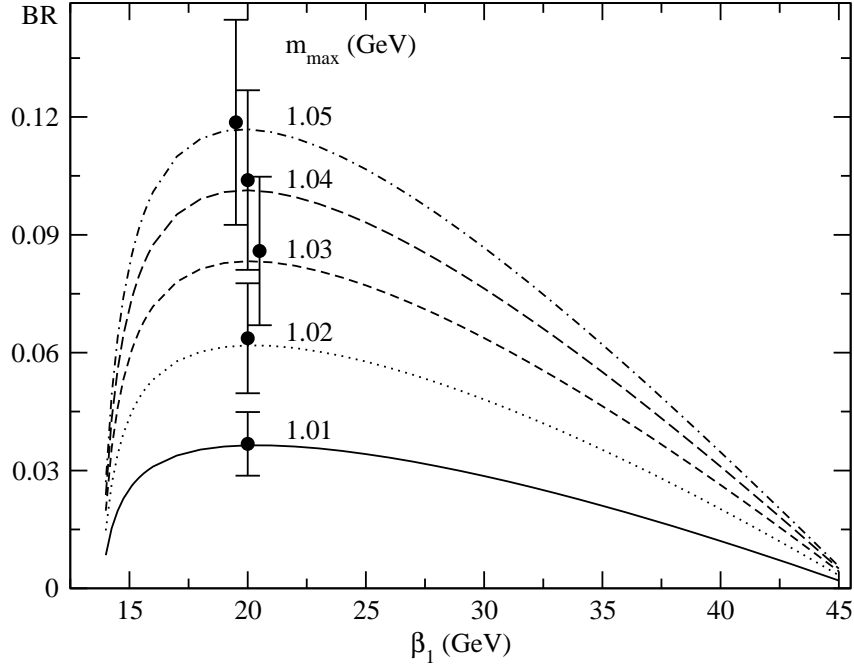


Fig. 1: Model dependence of the $K\bar{K}$ to $\pi\eta$ branching ratio on the range parameter β_1 . Points with errors are calculated BR values using the modified Flatté formula for the parameters of Ref. [6]. The upper effective mass integration limit is denoted by m_{\max} .

The Particle Data Group [4] has calculated an average branching ratio from the results obtained by the Crystal Barrel Collaboration[6] ($BR = 0.23 \pm 0.05$) and by the WA102 Group [32] ($BR = 0.166 \pm 0.01 \pm 0.02$). However, this procedure has to be taken with a great care since the value of BR depends very much on the integral limits. For the $p\bar{p}$ annihilation at rest into $\pi^0\pi^0\eta$ the available $\pi\eta$ effective mass varies between 682 MeV at the $\pi^0\eta$ threshold and the maximum value of about 1741 MeV. The WA102 Collaboration has studied the reaction $pp \rightarrow pf_1(1285)p$ with a subsequent decay of $f_1(1285)$ into the $\pi\pi\eta$ system. Then the maximum of the $\pi\eta$ effective mass equals to about 1147 MeV. We have recalculated the Crystal Barrel result 0.23 ± 0.05 , corresponding to $m_{\max} = 1741$ MeV, by lowering the upper limit to $m_{\max} = 1147$ MeV. Then the number $BR = 0.19 \pm 0.04$ was quite close to the WA102 result cited above. Encouraged by this agreement we have made calculations restricting m_{\max} limit to values closer to the $K\bar{K}$ threshold where the $a_0(980)$ resonance dominates. The results are shown in Fig. 1 by points with errors corresponding to the Crystal Barrel error $(0.05/0.23) \cdot 100\% = 22\%$. A comparison with the

theoretical curves following from our model indicates that the β_1 value should be chosen close to 20 GeV. Then the complete set of the potential parameters corresponding to the $a_0(980)$ lying on sheet II and the $a_0(1450)$ located on sheet III is following:

$$\begin{aligned}
\Lambda_{11} &= 2\beta_1^3\lambda_{11} = -0.032321, \\
\beta_1 &= 20.0 \text{ GeV}, \\
\Lambda_{22} &= 2\beta_2^3\lambda_{22} = -0.068173, \\
\beta_2 &= 21.831 \text{ GeV} \quad \text{and} \\
\Lambda_{12} &= 2(\beta_1\beta_2)^{3/2}\lambda_{12} = 5.0152 \cdot 10^{-4}.
\end{aligned} \tag{19}$$

4 Predictions

4.1 $K\bar{K}/\pi\eta$ branching ratio

Having established all the model parameters we can predict the $K\bar{K}/\pi\eta$ branching ratio in the $a_0(1450)$ mass range. One can take equal limits $m_1 = m_2$ and the $a_0(1450)$ width $\Gamma = 265$ MeV [4]. For a typical range of m between $m_1 \approx 1474 \text{ MeV} - \Gamma/2 \approx 1340 \text{ MeV}$ and $m_{max} \approx 1474 \text{ MeV} + \Gamma/2 \approx 1605 \text{ MeV}$ the branching ratio equals to 0.98. If we take wider limits like $m_1 = 1300 \text{ MeV}$ and $m_{max} = 1741 \text{ MeV}$, then the corresponding value is 0.78. The Crystal Barrel Collaboration result [6] $BR = 0.88 \pm 0.23$ agrees quite well with both theoretical numbers following from our model. Thus there is a mutual consistency of two branching ratios calculated within our model for the $a_0(980)$ and $a_0(1450)$ mesons and the experimental numbers obtained by the Crystal Barrel Collaboration.

Let us discuss for a moment the case when the $a_0(980)$ pole is fixed on sheet III at $M_2 - i\Gamma_2/2 = (985 - 46i) \text{ MeV}$ (see Eq. (14)). If we calculate the branching ratio BR as in Fig. 1 then the theoretical curves lie substantially lower (by a factor at least 2.5) than the recalculated experimental values. Thus in the following text this case will not be considered.

We have also studied a dependence of the $a_0(980)$ branching ratio on the input values of the $a_0(1450)$ mass and width. Let us recall that the OBELIX Collaboration has observed the $a_0(1300)$ resonance at $M = 1290 \text{ MeV}$ and $\Gamma = 80 \text{ MeV}$ [7]¹. If in our model we take the above values of M and Γ instead of $M = 1474 \text{ MeV}$ and $\Gamma = 265 \text{ MeV}$ then the resulting $a_0(980)$ branching ratio is too small by a factor at least 3 for both positions of $a_0(980)$ in (14) when it is compared with numbers represented by experimental points

¹The OBELIX Collaboration has determined the $a_0(980)$ branching ratio as 0.26 ± 0.06 [33] in agreement with the Crystal Barrel Collaboration ratio 0.23 ± 0.05 .

in Fig. 1. Even if the $a_0(980)$ mass would be lowered to 975 MeV as given in [7] then the $a_0(980)$ branching ratio should be even smaller. Hence we have found that, using our two channel model, it is difficult to link the parameters of the $a_0(980)$ and the $a_0(1300)$ resonances obtained by the OBELIX Collaboration.

4.2 Poles and zeroes

The relations (11) between the Jost function and the S-matrix elements are very useful in analysis of the positions of the S-matrix poles and zeroes in the complex planes of momenta k_1 and k_2 . A configuration of the poles and zeroes nearest to the physical region is important to understand a behaviour of the scattering amplitudes

$$T_{ij} = \frac{S_{ij} - \delta_{ij}}{2i}, \quad i, j = 1, 2. \quad (20)$$

The positions of the S-matrix poles corresponding to our choice (19) of model parameters are given in Table 1 and graphically presented in Fig. 2.

Table 1: Positions of the S-matrix poles (in units of MeV)

pole	ReE	ImE	Rek_1	Imk_1	Rek_2	Imk_2
1	1005.0	-24.5	336.6	-16.9	-94.5	65.2
2	991.5	-33.6	327.4	-23.3	85.4	-97.5
3	1474.0	-132.5	628.2	-76.4	546.9	-89.3
4	1467.3	-6.9	623.4	4.0	-539.1	-4.7

One can see that in addition to two postulated poles (1 and 3) the other two poles (2 and 4) are present. Near the $K\bar{K}$ threshold two poles (1 and 2) play an important role but the additional pole 4, related to $a_0(1450)$, lies far from the physical region. It does not mean, however, that this pole has no influence on the scattering amplitudes near 1450 MeV. In fact, every zero of the Jost function has a twin zero which lies symmetrically with respect to the imaginary momentum axis in both planes. This fact results from the general relation $D(k_1, k_2) = D^*(-k_1^*, -k_2^*)$ satisfied by the Jost function. Thus a zero of the S_{22} element² corresponding to a twin pole related to the pole 4 is localised very close and slightly above the physical axis in the $K\bar{K}$ plane. Similarly in the $\pi\eta$ complex momentum plane a zero of the S_{11} corresponding to the pole 4 lies slightly below the real axis and has an important influence on the $\pi\eta$ scattering amplitude.

²actually equivalent to a zero of $D(k_1, -k_2)$

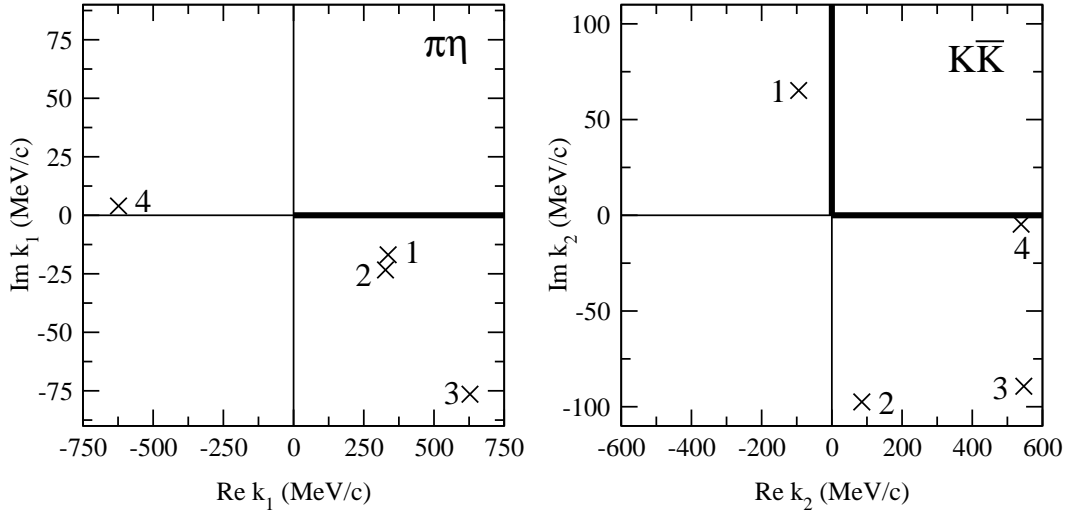


Fig. 2: Configuration of the S-matrix poles (denoted by crosses) in the $\pi\eta$ and $K\bar{K}$ channels. Poles 1 and 2 correspond to $a_0(980)$ and poles 3 and 4 correspond to $a_0(1450)$. The solid lines indicate the physical region.

4.3 Scattering amplitudes

Both the $K\bar{K}$ and $\pi\eta$ elastic scattering amplitudes are plotted in Fig. 3 in a form of Argand diagrams. Let us notice that a small circle of the $K\bar{K}$ amplitude

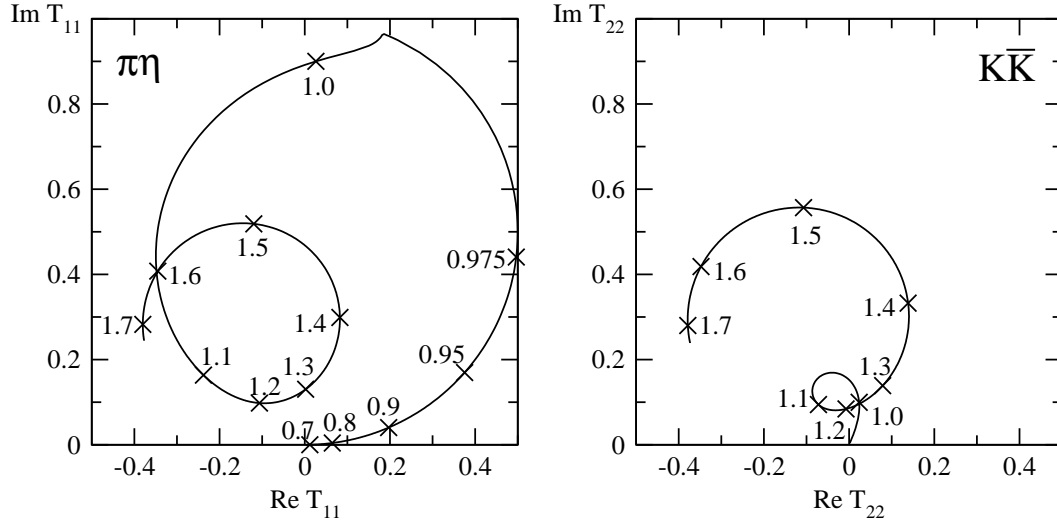


Fig. 3: Argand diagrams for the $\pi\eta$ and $K\bar{K}$ elastic scattering amplitudes. Numbers denote effective mass in units of GeV.

can be explained by a partial cancellation of the opposite contributions coming from two poles 1 and 2 related to the $a_0(980)$. The $\pi\eta$ results presented in Fig. 3 can be compared with the Argand plots of Weinstein and Isgur [8] and Törnqvist [9]. Qualitatively a shape of the $\pi\eta$ elastic amplitude is in agreement with Fig. 9a of [8] although the inelasticity parameter is larger in our $\pi\eta$ amplitude above the $K\bar{K}$ threshold. Also at higher effective $\pi\eta$ masses one sees differences which may be partially explained by another mass of the second a_0 meson, taken in Ref. [8], namely 1300 MeV, in comparison with our present value 1474 MeV. The $\pi\eta$ amplitude presented by Törnqvist seems to be quite similar to our amplitude up to the $K\bar{K}$ threshold but above it one can notice a different behaviour. The most characteristic difference is a lack of a circle related to the $a_0(1450)$ on his Argand plot (Fig. 6a in Ref. [9]).

The $K\bar{K}$ elastic amplitude plotted in Fig. 9a of Ref. [8] is also not similar to our $K\bar{K}$ amplitude. The inelasticity parameter η in Fig. 3 at the position of the $a_0(1450)$ resonance is close to zero. This is not a case at the end point above 1400 MeV on the curve presented in Ref. [8]. Briefly, the coupling of the $a_0(980)$ to $K\bar{K}$ is stronger in the model of Weinstein and Isgur than in our model. The opposite relation exists for the $a_0(1450)$ meson.

We have performed calculations of the production amplitudes which are inversely proportional to the Jost function. Results for the $\pi\eta$ production amplitudes are in qualitative agreement with those plotted in Figs. 4b and 8b by Bugg, Anisovich, Sarantsev and Zou for the reaction $p\bar{p} \rightarrow \eta\pi\pi$ [34].

4.4 Coupling constants

In Table 2 we give values of the coupling constants calculated at four poles 1 to 4 defined as in Eq. (34) of [35]. The ratio $|g_2^2/g_1^2|$ of the $a_0(980)$ coupling constants is equal to 0.72 at the pole 1 and 0.80 at the pole 2. Both numbers are smaller than the value $r = 1.03$ found by the Crystal Barrel Collaboration. Thus the width difference $\Gamma_2 - \Gamma_1 = 18$ MeV (seen in Table 1) is smaller than the value $\Gamma_2 - \Gamma_1 = 43$ MeV following from Eq. (14). However, the production amplitudes calculated within our model are in good agreement with the amplitudes obtained in [6] using the modified Flatté formula in the invariant mass range up to 1.05 GeV. Moduli of the coupling constants corresponding to the $a_0(1450)$ poles are stronger than the $a_0(980)$ coupling constants which can explain a considerably larger width of the $a_0(1450)$ than the width of the $a_0(980)$.

Despite of the closed values of the coupling constants at the poles 1 and 2, corresponding to the resonance $a_0(980)$, one should not average their values since these two poles are not symmetrically located, with respect to the origin, in the complex plane of the $K\bar{K}$ momentum k_2 (Fig. 2). The same remark is

Table 2: Moduli of the coupling constants $\left|\frac{g_i^2}{4\pi}\right|$ in GeV^2

channel	$a_0(980)$		$a_0(1450)$	
	1	2	3	4
$\pi\eta$	0.356	0.360	0.865	0.887
$K\bar{K}$	0.256	0.287	1.078	1.139

true for the poles 3 and 4 corresponding to the $a_0(1450)$.

4.5 Decoupled channels

Let us now consider a limit of the uncoupled $\pi\eta$ and $K\bar{K}$ channels in which the interchannel coupling constant λ_{12} goes to zero. We can gradually diminish

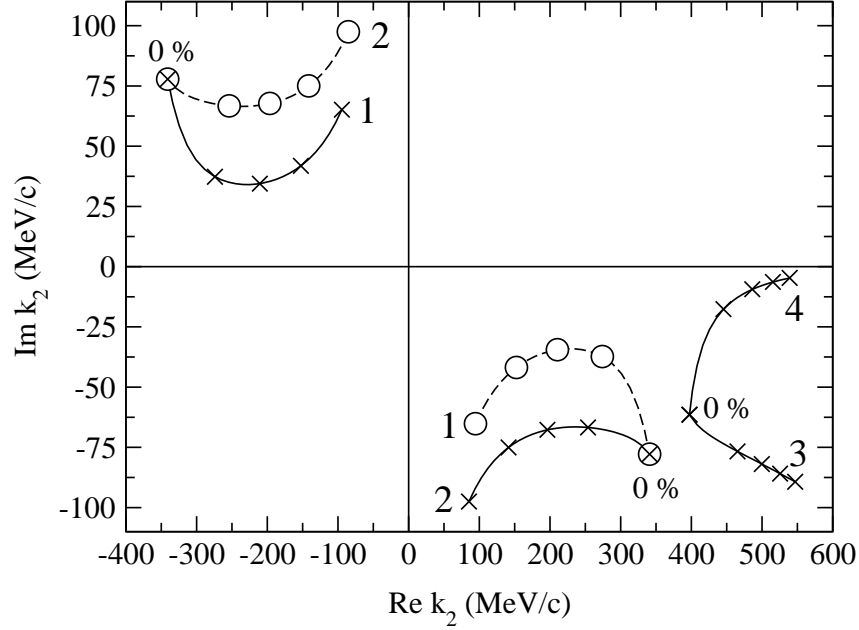


Fig. 4: Trajectories of four S-matrix poles in $K\bar{K}$ complex momentum plane (solid lines). Dashed lines correspond to trajectories of two zeroes of the S_{22} matrix element related to $a_0(980)$. Crosses and circles on trajectories indicate points of a reduction of the interchannel coupling λ_{12}^2 by 25% steps down to $\lambda_{12}^2 = 0$ (0%).

λ_{12} from its fitted value to a zero and observe trajectories of four poles (see Fig. 4). One can notice that in the limit $\lambda_{12} \rightarrow 0$ two poles 3 and 4 meet together

in the complex plane of k_2 momentum which means that in the uncoupled $K\bar{K}$ channel there exist a $K\bar{K}$ resonance at the effective mass equal to $(1270.1 - 76.9i)$ MeV. This $K\bar{K}$ resonance evolves into the $a_0(1450)$ when the coupling between channels is switched on.

Behaviour of the $a_0(980)$ poles is completely different. The pole 1 corresponding to the $a_0(980)$ on sheet $-+$ meets the trajectory end of the S_{22} zero related to the secondary pole 2³. Below the real axis the pole 2 moves to a point where it meets the S_{22} zero related to the pole 1. Thus effectively both poles 1 and 2 disappear from the $K\bar{K}$ channel in the limit of the vanishing inter-channel coupling constant. In the $\pi\eta$ channel the poles 1 and 2 meet together in this limit at one point, so for the parameter set (19) the $a_0(980)$ state has its origin in the $\pi\eta$ channel as a resonance at the effective mass $(1199.7 - 88.5i)$ MeV.

In such a way one can show that although the $K\bar{K}$ forces in the $I = 1$ S-wave are attractive ($\lambda_{22} < 0$ in (19)) they are not sufficiently strong to form a bound $K\bar{K}$ state. This information about the nature of the $a_0(980)$ meson can be confronted with the results obtained in literature on two close scalars $f_0(980)$ and $a_0(980)$. In [35] one can find different solutions for the $\pi\pi$, $K\bar{K}$ and 4π amplitudes fitted to the same experimental data. However, the data near the $K\bar{K}$ threshold are not yet precise enough to state whether the attractive $K\bar{K}$ forces in the isoscalar S-wave can always create a bound $f_0(980)$ state⁴. This result is at variance with a statement of Weinstein and Isgur [8] that both $f_0(980)$ and $a_0(980)$ are the bound $K\bar{K}$ states. We agree, however, with the conclusion of Janssen, Pearce, Holinde and Speth [11] that the $a_0(980)$ meson is not a bound $K\bar{K}$ state.

We have studied to what extent the conclusion about nonexistence of the $K\bar{K}$ bound state in the isovector S-wave remains valid in the limit of vanishing coupling constant between $\pi\eta$ and $K\bar{K}$ channels while simultaneously the input parameters like the masses and the widths of the $a_0(980)$ and $a_0(1450)$ are modified. We have checked that this is true if the $a_0(980)$ mass on sheet II changes between 950 MeV and 1020 MeV, its width varies between 25 and 100 MeV, the $a_0(1450)$ mass on sheet III changes between 1300 MeV and 1550 MeV and its width varies between 150 MeV and 350 MeV. In order to check possible large systematic errors of the input and to verify that the conclusion is firm the above limits are chosen larger than the errors of the a_0 resonance parameters given by the Particle Data Group.

³Zeros of the S_{22} matrix element at (k_1, k_2) are related to the poles of S_{22} at $(k_1, -k_2)$ and vice versa (see Eqs. (11)).

⁴However, the $K\bar{K}$ coupling constants of the $f_0(980)$ are much larger than the $K\bar{K}$ constants of the $a_0(980)$. They can attain values close to 2 GeV^2 in comparison with values below 0.3 GeV^2 shown in Table 2.

5 Conclusions

In summary, we have constructed the coupled channel model of two a_0 resonances decaying into the $\pi\eta$ and $K\bar{K}$ mesons. The parameters of the separable potentials have been fitted to experimental values of the a_0 masses and widths and to the $K\bar{K}/\pi\eta$ branching ratio near the $K\bar{K}$ threshold. Then we have predicted the $a_0(1450)$ branching ratio and verified that it was in agreement with the result of the Crystal Barrel Collaboration. The discrepancy in the interpretation of the $a_0(980)$ resonance mass position between the Crystal Barrel Collaboration and the E852 Group has been explained. The $a_0(980)$ resonance can be described by two poles near the $K\bar{K}$ threshold lying on sheets II and III. These two poles have substantially different widths when the production amplitudes are interpreted using the Flatté model with non vanishing $K\bar{K}$ coupling constant. In our model with parameters fixed by the present experimental data the $a_0(980)$ state cannot be interpreted as a bound $K\bar{K}$ state.

References

- [1] Proceedings of the 8-th Int. Conf. on Hadron Spectroscopy HADRON'99, Beijing, China, 24-28 Aug. 1999, edited by W. G. Li, Y. Z. Huang, B. S. Zou, Nucl. Phys. A675 (2000).
- [2] F. E. Close, hep-ph/0110081.
- [3] L. Montanet, Nucl. Phys. B (Proc. Suppl.) 86 (2000) 381.
- [4] D. E. Groom, *et al.*, (Particle Data Group), Eur. Phys. J. C15 (2000) 1.
- [5] S. Teige, *et al.*, (E852 Coll.), Phys. Rev. D59 (1999) 012001.
- [6] A. Abele, *et al.*, (Crystal Barrel Coll.), Phys. Rev. D57 (1998) 3860.
- [7] A. Bertin, *et al.*, (OBELIX Coll.), Phys. Lett. B434 (1998) 180.
- [8] J. Weinstein, N. Isgur, Phys. Rev. D41 (1990) 2236.
- [9] N. A. Törnqvist, Z. Phys. C68 (1995) 647.
- [10] R. L. Jaffe, Phys. Rev. D15 (1977) 267.
- [11] G. Janssen, B. C. Pearce, K. Holinde, J. Speth, Phys. Rev. D52 (1995) 2690.

- [12] K. Maltman, Phys. Lett. B462 (1999) 14.
- [13] N. N. Achasov, Nucl. Phys. A675 (2000) 279c.
- [14] A. Abele, *et al.*, (Crystal Barrel Coll.), Phys. Lett. B404 (1997) 179.
- [15] D. Alde, *et al.*, (GAMS Coll.), Yad. Phys. 62 (1999) 462.
- [16] D. Barberis, *et al.*, (WA102 Coll.), Phys. Lett. B488 (2000) 225.
- [17] J. Weinstein, Phys. Rev. D47 (1993) 911.
- [18] J. A. Oller, E. Oset, Nucl. Phys. A620 (1997) 438;
J. A. Oller, E. Oset, Nucl. Phys. A652 (1999) 407, Erratum.
- [19] D. Black, A. H. Fariborz, J. Schechter, Phys. Rev. D61 (2000) 074030.
- [20] R. Kamiński, L. Leśniak, K. Rybicki, Z. Phys. C74 (1997) 79.
- [21] R. Kamiński, L. Leśniak, K. Rybicki, hep-ph/0109268, accepted for publication in Eur. Phys. J. C.
- [22] F. E. Close, A. Kirk, Phys. Lett. B515 (2001) 13.
- [23] B. Kerbikov, F. Tabakin, Phys. Rev. C62 (2000) 064601.
- [24] O. Krehl, R. Rapp, J. Speth, Phys. Lett. B390 (1997) 23.
- [25] M. N. Achasov, *et al.*, Phys. Lett. B479 (2000) 53.
- [26] R. R. Akhmetshin, *et al.*, (CMD-2 Coll.), Phys. Lett. B462 (1999) 380.
- [27] A. Aloisio, *et al.*, (KLOE Coll.), hep-ex/0107024.
- [28] L. Leśniak, Acta Phys. Pol. B27 (1996) 1835.
- [29] R. Kamiński, L. Leśniak, J.-P. Maillet, Phys. Rev. D50 (1994) 3145.
- [30] S. M. Flatté, Phys. Lett. B63 (1976) 224.
- [31] C. Amsler, *et al.*, (Crystal Barrel Coll.), Phys. Lett. B333 (1994) 277.
- [32] D. Barberis, *et al.*, (WA102 Coll.), Phys. Lett. B440 (1998) 225.
- [33] S. Vecchi, *et al.*, (OBELIX Coll.), Nucl. Phys. A663 & 664 (2000) 613c.
- [34] D. V. Bugg, V. V. Anisovich, A. Sarantsev, B. S. Zou, Phys. Rev. D50 (1994) 4412.
- [35] R. Kamiński, L. Leśniak, B. Loiseau, Eur. Phys. J. C9 (1999) 141.